EASR

Engineering and Applied Science Research

https://www.tci-thaijo.org/index.php/easr/index

Published by the Faculty of Engineering, Khon Kaen University, Thailand

# Tailoring mechanical, thermophysical and ultrasonic properties of dysprosium monochalcogenides

Anurag Singh*[1, 2], Sudhanshu Tripathi[3], Devraj Singh[1] and Bhawan Jyoti[1]

[1]Department of Physics, Prof. Rajendra Singh (Rajju Bhaiya) Institute of Physical Sciences for Study and Research, Veer Bahadur Singh Purvanchal University, Jaunpur, 222003, India
[2]Department of Physics, Dr. Shyama Prasad Mukherjee Government Degree College, Bhadohi, 221401, India
[3]Department of IT and Engineering, Amity University, Tashkent, 100028, Uzbekistan

Received 26 September 2023
Revised 26 February 2024
Accepted 22 March 2024

**Abstract**

The ultrasonic characteristics of dysprosium monochalcogenides, DyX (X = S, Se and Te) as a function of temperature and crystallographic direction, are studied in present investigation. First, the second- and third-order elastic constants (SOECs and TOECs) have been computed using Coulomb and Born-Mayer potential from 0K to 500K. The mechanical properties have been evaluated with the achieved values of SOECs for finding the intrinsic properties, stability and futuristic performance of DyX. The mechanical stability and elastic moduli follow the order DyS > DySe > DyTe. Supplemental the acoustic velocities including Debye average velocity, thermal relaxation time, Debye temperature and nonlinear parameter have been computed along <100>, <110> and <111> directions in the temperature range 100K to 500K. The Debye average velocity is found to be highest for wave propagating along <110> and polarized along $<1\bar{1}0>$. Finally, the ultrasonic attenuation using the modified Mason's approach has been computed in the temperature regime 100-500K along different crystallographic directions and calculated results predict that Akheiser damping dominates over the thermal attenuation. The obtained results have been analyzed and discussed with the available literature.

**Keywords:** Monochalcogenides, Elastic constants, Thermal conductivity, Ultrasonic attenuation

## 1. Introduction

The transition metal chalcogenides have gained the much attention among material scientists and engineers because of their attractive structural, magnetic, electronic, thermal and electrical properties. The rare earth monochalcogenides are very much useful for material devices of spintronics. Many researchers have studied the elastic, structural, electronic, mechanical and thermophysical properties of rare-earth monochalcogenides and monopnictides [1-17]. The rock salt structured rare-earth pnictides and chalcogenides have been investigated by Petit et al. [1]. The structural, electronic and mechanical properties of DyX compounds were studied by Tripathi et al. [2] using first principles investigation. The metallic properties of these compounds have been predicted on the basis of the band structures, density of states and magnetic moments. Hulliger et al. [3] predicted that DyS, DySe, HoS and HoSe exhibit a type II antiferromagnetic order below the Neel temperature. The experimental and theoretical investigation of optical parameters of dysprosium pnictides were investigated by Schoenes et al. [4]. The influence of high pressure on elastic and mechanical parameters for rare-earth monochalcogenides have been performed by Gaith [5]. Bhajanker et al. [6] investigated the high pressure physical and thermal properties of DyP and DyAs. A first principles study of the 2-D Bi-based chalcogenides $Bi_2X_3$(X=S,Se,Te) monolayers with the orthorhombic structure has been predicted by Bafekry et al. [7]. The major advantage of monochalcogenides compounds is its scope in the fabrication of supercomputing machines and spintronic devices [8]. To explore the advantages of monochalcogenides, Otero-Diaz et al. [9] have studied thermal behaviour and microstructural characterization of γ-$Dy_2S_3$. Applications of monochalcogenides have been studied by various research investigators. Pokrzywnicki [10] have been predicted crystal field effects and magnetic properties of $Dy_2Te_3$. Khot et al. [11] have investigated synthesis of reduced graphene oxide dysprosium selenide composite electrode for energy storage. The synthesis, properties and applications of germanium chalcogenides have been presented by Privitera [12]. The thermoelectric performance of β-$PdX_2$ (X= S, Se, Te) monolayers with promising potential for thermoelectric applications has been studied with first-principle methods and Boltzmann transport theory by Ning et al. [13]. The temperature dependent ultrasonic attenuation in monochalcogenides SnTe, EuSe and CdO semiconductors due to phonon-phonon interaction and thermorelaxation mechanisms has been investigated along <100>, <110> and <111> crystallographic directions by Singh et al. [14]. Lahourpour et al. [15] have been investigated electronic, structural and optical parameters of graphene like nano-layers $MoX_2$ which confirms semiconductor behaviour of the $MoX_2$ nano layers with the direct band gap for S, Se and Te. Various studies on high magnetic ordering and valence behaviour predicted that these materials are very much useful for modulators and magneto-optic memory devices [16]. The electronic band-edges of lead chalcogenides and tin chalcogenides are investigated by Dantas et al. using the first principle computation [17].

*Corresponding author.
Email address: anuragrajpoot440@gmail.com
doi: 10.14456/easr.2024.32

Various elastic and mechanical parameters like shear modulus, Young modulus, bulk modulus, Poisson's ratio, Zener anisotropy ratio and Pugh's parameter are very much useful for determining the nature and quality of solids with respect to external stress [18, 19]. The SOECs as linear elastic parameters are the function of stress and strain [20]. TOECs are nonlinear elastic constants which give important findings about the mechanical strength of material, nonlinearity, nature of atomic bonding, and interionic potentials [21]. The anisotropic natures of these elastic parameters are very crucial to understand the thermophysical characteristics of materials and also, very much useful in the development of industrial apparatus with required physical properties under ambient conditions.

This motivate the authors to investigate the influence of temperature and orientation on SOECs and TOECs, Young's modulus (*Y*), bulk modulus (*B*), shear modulus (*G*), Cauchy's pressure ($C_p$), Poisson ratio ($\sigma$), Pugh's ratio (*B/G*), Zener anisotropy ratio ($A_n$), ultrasonic velocities and ultrasonic attenuation of the chosen DyX. The obtained results have been analyzed and compared with similar type of materials.

## 2. Theoretical approach

The temperature dependent second- and third-order elastic constants (SOECs and TOECs) are found out using Coulomb and Born-Mayer potential for the dysprosium monochalcogenides [22]. The interionic potential is given as

$$\Phi(R) = \Phi(C) + \Phi(B) \tag{1}$$

Where $\Phi(C)$ is the attractive electrostatic potential and $\Phi(B)$ is the short-range potential, which are defined as

$$\Phi(B) = A\,exp\left(\frac{-r}{b}\right) \text{ and } \Phi(C) = \pm\left(\frac{e^2}{r}\right) \tag{2}$$

Where *r* stands for nearest neighbour distance, *e* is the electronic charge, *b* is hardness parameter and *A* is the strength parameter. The temperature dependent SOECs and TOECs can be obtained by

$$C_{IJ} = C_{IJ}^0 + C_{IJ}^{Vib} \text{ and } C_{IJK} = C_{IJK}^0 + C_{IJK}^{Vib} \tag{3}$$

Where the superscript *0* stands for static part of elastic energy at absolute zero and '*vib*' stands for the vibrational energy at given temperature. The detailed expressions to evaluate the temperature dependent higher order elastic constants are given below [23].

### Static SOECs and TOECs Constants $C_{ij}^0$ and $C_{ijk}^0$

$$C_{11}^0 = \frac{3e^2}{2r_0^4}S_5^{(2)} + \frac{1}{br_0}\left(\frac{1}{r_0}+\frac{1}{b}\right)\varphi(r_0) + \frac{2}{br_0}\left(\frac{1}{\sqrt{2}r_0}+\frac{1}{b}\right)\varphi(\sqrt{2}r_0)$$

$$C_{12}^0 = C_{44}^0 = \frac{3e^2}{2r_0^4}S_5^{(1,1)} + \frac{1}{br_0}\left(\frac{1}{\sqrt{2}r_0}+\frac{1}{b}\right)\varphi(\sqrt{2}r_0)$$

$$C_{111}^0 = -\frac{15e^2}{2r_0^4}S_7^{(3)} - \left(\frac{3}{r_0^2}+\frac{3}{br_0}+\frac{1}{b^2}\right)\varphi(r_0) - \frac{1}{b}\left(\frac{3\sqrt{2}}{r_0^2}+\frac{6}{br_0}+\frac{2\sqrt{2}}{b^2}\right)\varphi(\sqrt{2}r_0)$$

$$C_{112}^0 = C_{166}^0 = -\frac{15e^2}{2r_0^4}S_5^{(2,1)} - \frac{1}{4b}\left(\frac{3\sqrt{2}}{r_0}+\frac{6}{br_0}+\frac{2\sqrt{2}}{b^2}\right)\varphi(\sqrt{2}r_0) \quad C_{123}^0 = C_{144}^0 = C_{456}^0 = -\frac{15e^2}{2r_0^4}S_7^{(1,1,1)}$$

$$\varphi(r_0) = A\exp\left(-\frac{r_0}{b}\right) \text{ and } \varphi(\sqrt{2}r_0) = A\exp\left(-\frac{\sqrt{2}r_0}{b}\right)$$

The values of lattice sum are

$$S_3^{(1)} = -0.58252,\ S_5^{(2)} = -1.04622,\ S_5^{(1,1)} = 0.23185$$

$$S_7^{(3)} = -1.36852,\quad S_7^{(2,1)} = 0.16115,\ S_7^{(1,1,1)} = -0.09045$$

### Vibrational SOECs and TOECs Constants $C_{ij}^{Vib}$ and $C_{ijk}^{Vib}$

$$C_{11}^{Vib} = f^{(1,1)}G_1^2 + f^{(2)}G_2$$

$$C_{12}^{Vib} = f^{(1,1)}G_1^2 + f^{(2)}G_{1,1}$$

$$C_{44}^{Vib} = G_{1,1}\,f^{(2)}$$

$$C_{111}^{Vib} = f^{(1,1,1)}G_1^3 + 3f^{(2,1)}G_2\ G_1\ + f^{(3)}G_3$$

$$C_{112}^{Vib} = f^{(1,1,1)}G_1^3 + f^{(2,1)}G_1\ (2G_{1,1} + G_2\ ) + f^{(3)}G_{2,1}$$

$$C_{123}^{Vib} = f^{(1,1,1)}G_1^3 + 3f^{(2,1)}G_1\ G_{1,1} + f^{(3)}G_{1,1,1}$$

$C_{144}^{Vib} = f^{(2,1)}G_1\ G_{1,1} + f^{(3)}G_{1,1,1}$

$C_{166}^{Vib} = 3f^{(2,1)}G_1\ G_{1,1} + f^{(3)}G_{2,1}$

$C_{456}^{Vib} = f^{(3)}G_{1,1,1}$

Where, $f^{(2)} = f^{(3)} = \frac{\hbar\omega_0}{8r_0^3}\coth x$

$f^{(1,1)} = f^{(2,1)} = -\frac{\hbar\omega_0}{96r_0^3}\left\{\frac{\hbar\omega_0}{2K_BT\sinh^2 x} + \coth x\right\}$

$f^{(1,1,1)} = -\frac{\hbar\omega_0}{384r_0^3}\left\{\frac{(\hbar\omega_0)^2\coth x}{6(K_BT)^2\sinh^2 x} + \frac{\hbar\omega_0\coth x}{2K_BT\sinh^2 x} + \coth x\right\}$

Here $X = \frac{\hbar\omega_0}{2k_BT}$; $\hbar = \frac{h}{2\pi}$ and $h$ is Planck's constant.

Expressions of $G_n$ are given by the following relations.

$G_1 = 2\left[\left(2 + 2\rho_0 - \rho_0^2\right)\varphi(r_0) + 2\left(\sqrt{2} + \left(2\rho_0 - \sqrt{2}\rho_0^2\right)\varphi(\sqrt{2}r_0)\right)\right]H$

$G_2 = 2\left[\left(-6 - 6\rho_0 - \rho_0^2 + \rho_0^3\right)\varphi(r_0) + \left(-3\sqrt{2} - 6\rho_0 - \sqrt{2}\rho_0^2 + 2\rho_0^3\right)\varphi(\sqrt{2}r_0)\right)\right]H$

$G_3 = \{30 + 30\rho_0 + 9\rho_0^2 - \rho_0^3 - \rho_0^4)\varphi(r_0)\ + (\frac{15}{2}\sqrt{2} + 15\rho_0 + \frac{9}{2}\sqrt{2}\rho_0^2 - \rho_0^3 - \sqrt{2}\rho_0^4)\varphi(\sqrt{2}r_0)\}H$

$G_{1,1} = \left[\left(-3\sqrt{2} - 6\rho_0 - \sqrt{2}\rho_0^2 + 2\rho_0^3\right)\varphi\left(\sqrt{2}r_0\right)\right]H$

$G_{2,1} = \left[\left(\frac{15}{\sqrt{2}} + 15\rho_0 + \frac{9}{\sqrt{2}}\rho_0^2 - \rho_0^3 - \sqrt{2}\rho_0^4\right)\varphi\left(\sqrt{2}r_0\right)\right]H$

$G_{1,1,1} = 0$

Where $H$ is given by the following expression

$H = \left[\left(\rho_0 - 2\right)\varphi(r_0) + 2\left(\rho_0 - \sqrt{2}\rho_0^2\right)\varphi(\sqrt{2}r_0)\right)\right]^{-1}$ and $\rho_0 = \frac{r_0}{b}$

To analyze strength, stability and nature of crystal, the elastic moduli of DyX like *Y, B, G, $C_p$, σ, $A_n$* and *B/G* has been calculated with the help of the expressions given in our recent work [24, 25].

The orientation dependent ultrasonic velocity is a decisive parameter for material characterization. The longitudinal velocity ($V_L$) and shear velocities of the ultrasonic waves ($V_{S1}$, $V_{S2}$) of acoustical waves along different directions are evaluated with the help of SOECs and density [26].

Along <100> direction-

$V_L = \sqrt{C_{11}/\rho}\ ;\ \ V_{S1} = V_{S2} = \sqrt{C_{44}/\rho};$

Along <111> direction

$V_L = \sqrt{(C_{11} + 2C_{12} + 4C_{44})/3\rho};\ V_{S1} = V_{S2} = \sqrt{(C_{11} - C_{12} + C_{44})/3\rho};$

Along <110> direction

$V_L = \sqrt{(C_{11} + C_{12} + 2C_{44})/2\rho};\ V_{S1} = \sqrt{C_{44}/\rho};\ V_{S2} = \sqrt{(C_{11} - C_{12})/\rho};$

Where $\rho$ stands for density.

The expression for finding the Debye temperature ($\theta_D$) is given below

$$\theta_D = \frac{h}{k_B}\left(\frac{3nN\rho}{4\pi M}\right)^{1/3} V_D \quad (4)$$

Where $h$ is the Planck's constant, $n$ is the number of atoms in a unit cell of lattice, $N$ is the Avogadro's number, $\rho$ is the density of cubic crystal, $k_B$ is the Boltzmann constant, $M$ is the molecular weight and $V_D$ is average Debye velocity. The ultrasonic attenuation due to phonon-phonon and thermal elastic relaxation mechanisms occurs at high temperature. Firstly, the theory for ultrasonic attenuation due to phonon-phonon mechanism interaction mechanism was proposed by Akhieser [27], so it is known as Akheiser loss for longitudinal and shears waves. Further Bömmel and Dransfeld [28] modified this mechanism. Finally, correct form of phonon viscosity mechanism has been presented by Mason [29]. The expressions to compute the loss due to Akheiser and thermorelaxation mechanism has been given in our recent work [23].

## 3. Results and discussion

The second- and third-order elastic constants are calculated with two parameters *i.e.* nearest-neighbour distance and the hardness constant in the temperature regime 0-500K. The nearest-neighbour distance for DyS, DySe and DyTe are 2.695 Å, 2.875 Å, 3.06 Å respectively [2] and hardness constant is 0.292 Å for all materials [30]. The computed results of SOECs and TOECs have been presented in Table 1 for DyX in the temperature range 0-500K.

**Table 1** SOECs and TOECs of DyX in temperature range 0-500K (in GPa)

| Material | Temp(K) | $C_{11}$ | $C_{12}$ | $C_{44}$ | $C_{111}$ | $C_{112}$ | $C_{123}$ | $C_{144}$ | $C_{166}$ | $C_{456}$ |
|---|---|---|---|---|---|---|---|---|---|---|
| DyS | 0 | 5.45 | 1.79 | 1.79 | -88.47 | -7.32 | 2.94 | 2.94 | -7.32 | 2.94 |
| | 100 | 5.72 | 1.71 | 1.80 | -90.16 | -7.02 | 2.47 | 2.96 | -7.37 | 2.94 |
| | 200 | 5.88 | 1.62 | 1.80 | -90.81 | -6.72 | 2.00 | 2.98 | -7.39 | 2.94 |
| | 300 | 6.07 | 1.54 | 1.81 | -91.68 | -6.41 | 1.54 | 3.01 | -7.42 | 2.94 |
| | 400 | 6.26 | 1.45 | 1.82 | -92.60 | -6.11 | 1.07 | 3.03 | -7.45 | 2.94 |
| | 500 | 6.46 | 1.37 | 1.83 | -93.55 | -5.80 | 0.60 | 3.05 | -7.48 | 2.94 |
| DySe | 0 | 5.01 | 1.46 | 1.46 | -83.40 | -5.97 | 2.45 | 2.45 | -5.97 | 2.45 |
| | 100 | 5.23 | 1.38 | 1.47 | -84.73 | -5.67 | 1.97 | 2.47 | -6.01 | 2.45 |
| | 200 | 5.41 | 1.30 | 1.48 | -85.54 | -5.36 | 1.50 | 2.49 | -6.03 | 2.45 |
| | 300 | 5.59 | 1.22 | 1.49 | -86.47 | -5.05 | 1.02 | 2.51 | -6.06 | 2.45 |
| | 400 | 5.78 | 1.14 | 1.49 | -87.42 | -4.74 | 0.54 | 2.53 | -6.08 | 2.45 |
| | 500 | 5.97 | 1.06 | 1.50 | -88.43 | -4.43 | 0.06 | 2.55 | -6.11 | 2.45 |
| DyTe | 0 | 4.35 | 1.08 | 1.08 | -75.44 | -4.35 | 1.85 | 1.85 | -4.35 | 1.85 |
| | 100 | 4.55 | 1.00 | 1.08 | -76.66 | -4.04 | 1.36 | 1.87 | -4.38 | 1.85 |
| | 200 | 4.72 | 0.92 | 1.09 | -77.52 | -3.73 | 0.87 | 1.88 | -4.40 | 1.85 |
| | 300 | 4.89 | 0.85 | 1.09 | -78.46 | -3.41 | 0.38 | 1.89 | -4.42 | 1.85 |
| | 400 | 5.07 | 0.77 | 1.09 | -79.41 | -3.10 | -0.10 | 1.91 | -4.44 | 1.85 |
| | 500 | 5.24 | 0.69 | 1.10 | -80.38 | -2.79 | -0.59 | 1.92 | -4.46 | 1.85 |

Table 1 states that the SOECs and TOECs have been found greatest for DyS and lowest for DyTe, which indicates that DyS has better fundamental characteristics than other DyX. Table 1 predicts that on increasing temperature SOECs $C_{11}$ increases and $C_{12}$ decrease with temperature for the DyX. The TOECs $C_{112}$, $C_{144}$ increases with temperature and $C_{111}$, $C_{166}$, $C_{123}$ decreas with temperature while $C_{456}$ remains constant. The values of second- and third-order elastic parameters of DyX do not exist in available literature, so the obtained results of SOECs and TOECs have been compared with available values of $B_1$ structured similar monochalcogenides materials like neptunium monochalcogenides [31], lanthanum monochalcogenides [32] praseodymium monochalcogenides [33] and fermium monopnictides [34]. The orders of the SOECs and TOECs have the same quantum. Our calculated values are nearly in close agreement with existing values with a variation of 5-10% which justifies our theoretical approach. The Cauchy's relations $C_{12}^0 = C_{44}^0$; $C_{112}^0 = C_{166}^0$; $C_{123}^0 = C_{456}^0 = C_{144}^0$ defined by Cousins [35] are satisfied at 0K in our case but do not hold good on higher temperature because vibrational part of energy affects the nature of interacting forces. The stability criterion [23] has been satisfied by SOECs of DyX which shows the mechanical stability of dysprosium monochalcogenides. The inequalities $C_{11} + 2C_{12} > 0$, $C_{11} - C_{12} > 0$ and $C_{44} > 0$ are satisfied in present case which shows that DyX are elastically stable at all temperatures. The computed values of TOECs are maximum for DyS and minimum for DyTe.

Figures 1-6 depicts the second- and third-order elastic constants with respect to temperature. Among total 9 elastic constants 3 elastic constants ($C_{11}, C_{112}, C_{144}$) are increasing and 4 elastic constants ($C_{12}, C_{111}, C_{166}, C_{123}$) are decreasing with temperature while $C_{44}$ is varying very slightly with temperature and $C_{456}$ is constant. $C_{123}$ shows maximum deviation with temperature. The increase or decrease in elastic constants is due to increase or decrease in atomic interaction with temperature. The computation of elastic constants consists of two parts i.e., static and vibrational part. The vibrational part of $C_{44}$ is minimum among SOECs that's why variation in $C_{44}$ is minimum and seems to be almost constant. For $C_{456}$ the calculated vibrational part is zero that's why $C_{456}$ is always constant with increase in temperature.

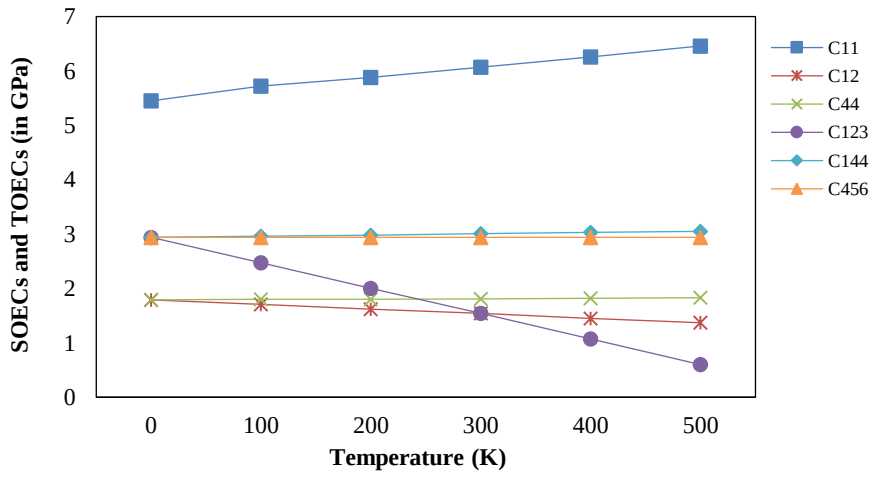


**Figure 1** The SOECs and TOECs of DyS with positive temperature gradient.

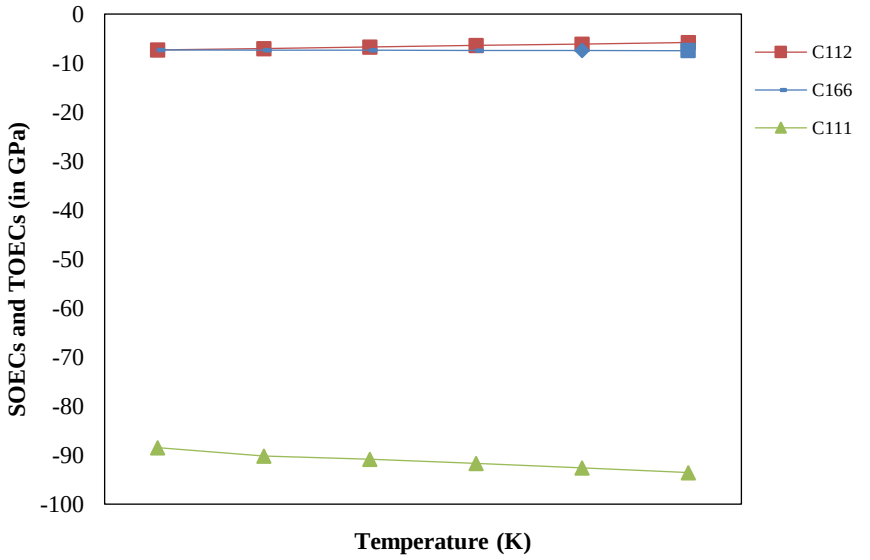


**Figure 2** The SOECs and TOECs of DyS with negative temperature gradient.

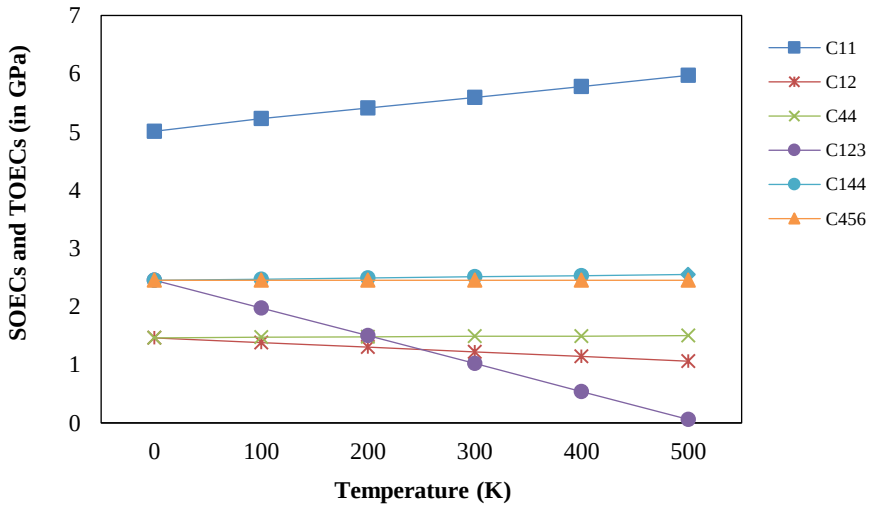


**Figure 3** The SOECs and TOECs of DySe with positive temperature gradient.

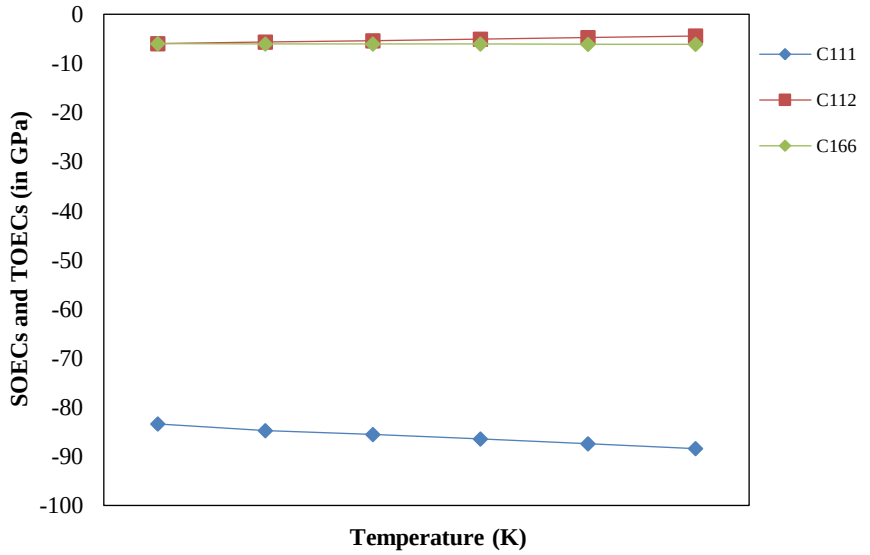


**Figure 4** The SOECs and TOECs of DySe with negative temperature gradient.

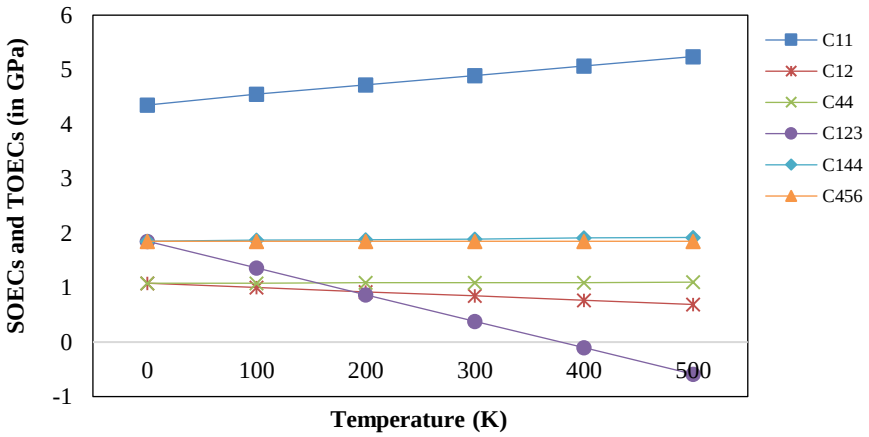


**Figure 5** The SOECs and TOECs of DyTe with positive temperature gradient.

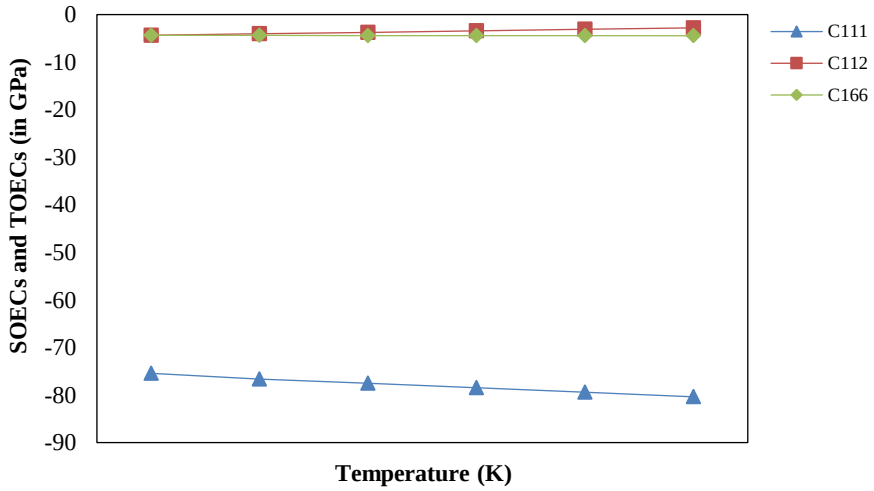


**Figure 6** The SOECs and TOECs of DyTe with negative temperature gradient.

The SOECs are further applied to calculate elastic moduli of DyX like bulk modulus (*B*), shear modulus (*G*), Young's modulus(*Y*), Cauchy pressure ($C_P$), Poisson's ratio ($\sigma$), Zener anisotropic parameter ($A_n$) and Pugh's indicator (*B/G*) at 300K and the computed values of these are placed in Table 2.

**Table 2** The mechanical parameters of DyX at room temperature.

| Material | *Y* (GPa) | *B* (GPa) | *G* (GPa) | $C_p$ (GPa) | $\sigma$ | $A_n$ | *B/G* |
|---|---|---|---|---|---|---|---|
| DyS | 47.84 | 30.54 | 19.84 | 22.66 | 0.23 | 0.80 | 1.54 |
| DySe | 42.83 | 26.83 | 17.35 | 21.83 | 0.23 | 0.68 | 1.57 |
| DyTe | 34.70 | 21.99 | 14.02 | 20.21 | 0.24 | 0.54 | 1.64 |

From Table 2 it is obvious that the values of mechanical constants for DyS is maximum and minimum for DyTe which predicts that DyS is more mechanically stable than other materials of DyX. The larger value of G for DyS indicates that DyS is much harder than DySe and DyTe. The fracture to toughness ratio i.e., Pugh's ratio (*B/G*) [36] is found below 1.75 which indicates that the selected dysprosium chalcogenides have brittle nature [37]. For non-central nature of inter atomic forces the Poisson's ratio limit is found between $0.3<\sigma<0.5$. In this work the evaluated values of the Poisson ratio are less than 0.3 which predicts that interionic forces are non-central in nature for DyX [38]. The Cauchy pressure ($C_p = C_{12} - C_{44}$) and Poisson's ratio ($\sigma$) are used to define the ductility and brittleness characteristics of the chosen monochalcogenides. For brittle materials the value of Cauchy pressure is negative while for ductile materials, it is positive. The Poisson's ratio limit for ductility is greater than 0.3 and for brittleness its limit is less than 0.3. For non-central characteristics of inter ionic bonding forces $\sigma$ should lie in between $0.2<\sigma<0.5$. From Table 2 it is obvious that values of $\sigma$ for dysprosium monochalcogenides are less than 0.3($\sigma< 0.3$) and $C_P$ is less than zero ($C_P < 0$) which confirms that DyX are brittle in nature and inter-ionic forces are non-central. The Zener anisotropy parameter ($A_n$) measures the degree of elastic anisotropy which should be equal to unity in case of isotropic materials. But the chosen DyX materials are anisotropic at all temperatures as the value of $A_n$ is less than 1.

Temperature and direction dependent ultrasonic velocities ($V_L$, $V_S$ and $V_D$) are calculated along <100>, <110> and <111> within temperatures range 100-500K. The calculated results of acoustic velocities and Debye temperature for DyX at different temperatures are given in Table 3.

**Table 3** Acoustic velocities ($10^3$ ms$^{-1}$) and Debye temperature $\theta_D$ (K) within temperature range 100-500K along different directions.

| Material | Direction of Propagation | Direction of Polarization | Velocity | 100K | 200K | 300K | 400K | 500K |
|---|---|---|---|---|---|---|---|---|
| DyS | <100> | <100> | $V_L$ | 2.64 | 2.68 | 2.72 | 2.76 | 2.81 |
| | | | $V_{S1}=V_{S2}$ | 1.48 | 1.48 | 1.49 | 1.49 | 1.49 |
| | | | $V_D$ | 1.65 | 1.65 | 1.66 | 1.67 | 1.67 |
| | | | $\theta_D$ | 365 | 365 | 367 | 369 | 369 |
| | <110> | <001> | $V_L$ | 2.59 | 2.61 | 2.62 | 2.63 | 2.65 |
| | | | $V_{S1}$ | 1.48 | 1.49 | 1.49 | 1.49 | 1.49 |
| | | <1$\bar{1}$0> | $V_{S2}$ | 2.21 | 2.28 | 2.35 | 2.42 | 2.49 |
| | | | $V_D$ | 1.87 | 1.89 | 1.90 | 1.92 | 1.93 |
| | | | $\theta_D$ | 413 | 418 | 420 | 424 | 427 |
| | <111> | <$\bar{1}$10> | $V_L$ | 2.58 | 2.58 | 2.58 | 2.59 | 2.59 |
| | | | $V_{S1}=V_{S2}$ | 1.54 | 1.57 | 1.61 | 1.64 | 1.68 |
| | | | $V_D$ | 1.70 | 1.74 | 1.77 | 1.81 | 1.84 |
| | | | $\theta_D$ | 376 | 385 | 391 | 400 | 407 |
| DySe | <100> | <100> | $V_L$ | 2.43 | 2.47 | 2.51 | 2.55 | 2.59 |
| | | | $V_{S1}=V_{S2}$ | 1.29 | 1.29 | 1.29 | 1.30 | 1.30 |
| | | | $V_D$ | 1.44 | 1.44 | 1.45 | 1.45 | 1.46 |
| | | | $\theta_D$ | 298 | 298 | 300 | 300 | 303 |
| | <110> | <001> | $V_L$ | 2.32 | 2.33 | 2.35 | 2.36 | 2.38 |
| | | | $V_{S1}$ | 1.29 | 1.29 | 1.29 | 1.30 | 1.30 |
| | | <1$\bar{1}$0> | $V_{S2}$ | 2.08 | 2.15 | 2.22 | 2.28 | 2.35 |
| | | | $V_D$ | 1.66 | 1.67 | 1.68 | 1.69 | 1.70 |
| | | | $\theta_D$ | 344 | 346 | 348 | 350 | 352 |
| | <111> | <$\bar{1}$10> | $V_L$ | 2.28 | 2.29 | 2.29 | 2.30 | 3.00 |
| | | | $V_{S1}=V_{S2}$ | 1.41 | 1.45 | 1.48 | 1.52 | 1.55 |
| | | | $V_D$ | 1.56 | 1.59 | 1.63 | 1.66 | 1.69 |
| | | | $\theta_D$ | 323 | 330 | 338 | 344 | 350 |
| DyTe | <100> | <100> | $V_L$ | 2.29 | 2.34 | 2.38 | 2.42 | 2.46 |
| | | | $V_{S1}=V_{S2}$ | 1.12 | 1.12 | 1.12 | 1.13 | 1.13 |
| | | | $V_D$ | 1.26 | 1.26 | 1.27 | 1.27 | 1.27 |
| | | | $\theta_D$ | 245 | 245 | 247 | 247 | 247 |
| | <110> | <001> | $V_L$ | 2.11 | 2.13 | 2.14 | 2.16 | 2.17 |
| | | | $V_{S1}$ | 1.12 | 1.12 | 1.12 | 1.13 | 1.13 |
| | | <1$\bar{1}$0> | $V_{S2}$ | 2.02 | 2.09 | 2.16 | 2.23 | 2.29 |
| | | | $V_D$ | 1.47 | 1.48 | 1.49 | 1.50 | 1.51 |
| | | | $\theta_D$ | 286 | 288 | 290 | 292 | 294 |
| | <111> | <$\bar{1}$10> | $V_L$ | 2.05 | 2.05 | 2.06 | 2.06 | 2.06 |
| | | | $V_{S1}=V_{S2}$ | 1.34 | 1.37 | 1.41 | 1.44 | 1.48 |
| | | | $V_D$ | 1.46 | 1.50 | 1.53 | 1.57 | 1.60 |
| | | | $\theta_D$ | 284 | 292 | 298 | 306 | 312 |

Longitudinal and shear ultrasonic velocities are calculated for DyX at temperatures 100-500K along three crystallographic axes <100>, <110>, <111> and polarized along <100>, <001>, <1$\bar{1}$0>, <$\bar{1}$10> directions. The ultrasonic velocity for longitudinal and shear mode depends on second order elastic constants and density of the chosen material. Table 3 predicts that ultrasonic velocities are increasing with increase in temperature because ultrasonic velocity depends on SOECs. The SOECs ($C_{11}$ and $C_{44}$) increases with increase in temperature for the chosen DyX as given in Table 1. The acoustic velocities ($V_L$ and $V_S$ both) are highest for DyS and lowest for DyTe because ultrasonic velocity is inversely proportional to density. The longitudinal ultrasonic velocity is maximum along <100> and minimum along <111> while shear ultrasonic velocity is maximum along <110> and minimum along <100> in case of chosen materials. The Debye average velocity decreases along <100> and increases along <110> for DyX. The Debye average velocity for DyS is higher than DySe and DyTe due to its lowest density and atomic weight than DySe and DyTe. The calculated values of acoustic velocities are of same order as of similar material [32, 33]. One of the important thermo-physical property is the Debye temperature which indicates most possible mode of wave propagation. The calculated values in Table 3 shows that the Debye temperature for DyS and DySe are highest along <110> direction while for DyTe it is highest along <111> direction due to dependence of Debye temperature on Debye velocity. Among the chosen materials the Debye temperature decreases DyS to DyTe and follow the order DyS > DySe > DyTe because Debye velocity is inversely proportional to molecular weight .The energy density ($E_0$) and the specific heat capacity per unit volume ($C_V$) are computed with $\theta_D/T$ tables of AIP Handbook [39].

The calculated values of ultrasonic attenuation constants due to thermal mechanism $(\alpha/v^2)_{th}$, Akhieser longitudinal damping $(\alpha/v^2)_L$, Akhieser shear damping $(\alpha/v^2)_S$, thermal relaxation time ($\tau_{th}$) and acoustical coupling constants $D_L$ & $D_S$, for DyS, DySe and DyTe with in temperature range 100-500K have been presented in Tables 4-6 respectively.

**Table 4** The temperature dependent $\tau_{th}$(in ps); $D_L$, $D_{S1}$, $D_{S2}$; $(\alpha/v^2)_{th}$, $(\alpha/v^2)_L$, $(\alpha/v^2)_{s1}$ and $(\alpha/v^2)_{s2}$ (all $(\alpha/v^2)$ in $10^{-15}$Nps$^2$m$^{-1}$) along ⟨100⟩, ⟨110⟩,⟨111⟩ for DyS

| Direction | Temp(K) | $\tau_{th}$ | $D_L$ | $D_{S1}$ | $D_{S2}$ | $(\alpha/v^2)_{th}$ | $(\alpha/v^2)_L$ | $(\alpha/v^2)_{S1}$ | $(\alpha/v^2)_{S2}$ |
|---|---|---|---|---|---|---|---|---|---|
| | 100 | 5.23 | 15.64 | 1.07 | 1.07 | 0.002 | 0.359 | 0.069 | 0.069 |
| ⟨100⟩ | 200 | 4.66 | 14.95 | 1.05 | 1.0 | 0.003 | 0.887 | 0.184 | 0.184 |
| | 300 | 4.57 | 14.08 | 1.04 | 1.04 | 0.004 | 1.280 | 0.290 | 0.290 |
| | 400 | 4.53 | 13.30 | 1.03 | 1.03 | 0.004 | 1.848 | 0.402 | 0.402 |
| | 500 | 4.53 | 12.59 | 1.02 | 1.02 | 0.005 | 1.902 | 0.511 | 0.511 |
| ⟨110⟩ | 100 | 4.33 | 17.60 | 27.77 | 1.04 | 0.006 | 0.310 | 0.049 | 0.0395 |
| | 200 | 4.27 | 17.60 | 26.55 | 1.01 | 0.011 | 0.955 | 0.038 | 0.0411 |
| | 300 | 3.97 | 16.52 | 25.37 | 0.98 | 0.015 | 1.417 | 5.937 | 0.058 |
| | 400 | 3.92 | 15.54 | 24.29 | 0.95 | 0.018 | 1.763 | 7.935 | 0.688 |
| | 500 | 3.90 | 14.65 | 23.29 | 0.93 | 0.020 | 2.217 | 9.813 | 0.084 |
| ⟨111⟩ | 100 | 5.03 | 17.35 | 18.88 | 18.88 | 0.004 | 0.402 | 1.031 | 1.031 |
| | 200 | 4.29 | 16.29 | 18.12 | 18.12 | 0.008 | 0.949 | 2.338 | 2.338 |
| | 300 | 4.08 | 14.98 | 17.39 | 17.39 | 0.011 | 1.399 | 3.380 | 3.380 |
| | 400 | 3.95 | 13.77 | 16.72 | 16.72 | 0.014 | 1.763 | 4.194 | 4.194 |
| | 500 | 3.84 | 12.69 | 16.12 | 16.12 | 0.016 | 2.031 | 4.769 | 4.769 |

**Table 5** The temperature dependent $\tau_{th}$(in ps); $D_L$, $D_{S1}$, $D_{S2}$;$(\alpha/v^2)_{th}$, $(\alpha/v^2)_L$, $(\alpha/v^2)_{S1}$ and $(\alpha/v^2)_{S2}$(all $(\alpha/v^2)$ in$10^{-15}$Nps$^2$m$^{-1}$) along⟨100⟩, ⟨110⟩,⟨111⟩ for DySe

| Direction | Temp (K) | $\tau_{th}$ | $D_L$ | $D_{S1}$ | $D_{S2}$ | $(\alpha/v^2)_{th}$ | $(\alpha/v^2)_L$ | $(\alpha/v^2)_{S1}$ | $(\alpha/v^2)_{S2}$ |
|---|---|---|---|---|---|---|---|---|---|
| ⟨100⟩ | 100 | 6.11 | 16.64 | 1.08 | 1.08 | 0.001 | 0.526 | 0.113 | 0.113 |
| | 200 | 5.67 | 15.78 | 1.06 | 1.06 | 0.003 | 1.209 | 0.283 | 0.283 |
| | 300 | 5.58 | 14.86 | 1.05 | 1.05 | 0.004 | 1.774 | 0.457 | 0.457 |
| | 400 | 5.57 | 14.02 | 1.04 | 1.04 | 0.005 | 2.223 | 0.627 | 0.627 |
| | 500 | 5.57 | 13.27 | 1.03 | 1.03 | 0.005 | 2.585 | 0.797 | 0.797 |
| ⟨110⟩ | 100 | 5.40 | 17.78 | 29.92 | 0.97 | 0.007 | 0.356 | 1.753 | 0.013 |
| | 200 | 4.89 | 18.45 | 28.52 | 0.95 | 0.013 | 1.373 | 6.265 | 0.045 |
| | 300 | 4.78 | 17.36 | 27.22 | 0.92 | 0.018 | 2.093 | 9.800 | 0.065 |
| | 400 | 4.77 | 16.35 | 26.04 | 0.90 | 0.022 | 2.728 | 13.13 | 0.082 |
| | 500 | 4.75 | 15.43 | 24.98 | 0.87 | 0.025 | 3.263 | 16.16 | 0.095 |
| ⟨111⟩ | 100 | 5.41 | 17.99 | 20.28 | 20.28 | 0.006 | 0.573 | 1.367 | 1.367 |
| | 200 | 4.79 | 16.74 | 19.41 | 19.41 | 0.011 | 1.316 | 3.015 | 3.015 |
| | 300 | 4.59 | 15.33 | 18.61 | 18.61 | 0.015 | 1.921 | 4.315 | 4.315 |
| | 400 | 4.42 | 14.04 | 17.90 | 17.90 | 0.019 | 2.378 | 5.226 | 5.226 |
| | 500 | 4.31 | 12.91 | 17.27 | 17.27 | 0.022 | 2.735 | 5.974 | 5.974 |

**Table 6** The temperature dependent $\tau_{th}$(ps); $D_L$, $D_{S1}$, $D_{S2}$; $(\alpha/v^2)_{th}$, $(\alpha/v^2)_L$, $(\alpha/v^2)_{s1}$ and$(\alpha/v^2)_{s2}$(all $(\alpha/v^2)$ in $10^{-15}$Nps$^2$m$^{-1}$) along⟨100⟩,⟨110⟩,⟨111⟩ for DyTe

| Direction | Temp (K) | $\tau_{th}$ | $D_L$ | $D_{S1}$ | $D_{S2}$ | $(\alpha/v^2)_{th}$ | $(\alpha/v^2)_L$ | $(\alpha/v^2)_{s1}$ | $(\alpha/v^2)_{s2}$ |
|---|---|---|---|---|---|---|---|---|---|
| ⟨100⟩ | 100 | 7.48 | 18.31 | 1.09 | 1.09 | 0.002 | 0.079 | 0.202 | 0.202 |
| | 200 | 7.13 | 17.26 | 1.08 | 1.08 | 0.003 | 1.726 | 0.487 | 0.487 |
| | 300 | 7.11 | 16.23 | 1.07 | 1.07 | 0.004 | 2.491 | 0.779 | 0.779 |
| | 400 | 7.10 | 15.30 | 1.07 | 1.07 | 0.005 | 3.091 | 1.067 | 1.067 |
| | 500 | 7.09 | 14.48 | 1.06 | 1.06 | 0.005 | 3.566 | 1.352 | 1.352 |
| ⟨110⟩ | 100 | 6.49 | 21.27 | 33.42 | 0.89 | 0.010 | 0.948 | 5.00 | 0.022 |
| | 200 | 6.06 | 20.23 | 31.82 | 0.87 | 0.017 | 2.188 | 11.71 | 0.049 |
| | 300 | 6.01 | 19.03 | 30.37 | 0.85 | 0.024 | 3.303 | 18.19 | 0.071 |
| | 400 | 5.99 | 17.92 | 29.09 | 0.83 | 0.028 | 4.243 | 24.11 | 0.088 |
| | 500 | 5.81 | 16.95 | 27.95 | 0.81 | 0.032 | 5.074 | 29.72 | 0.102 |
| ⟨111⟩ | 100 | 5.90 | 19.18 | 22.54 | 22.54 | 0.009 | 0.851 | 1.808 | 1.808 |
| | 200 | 5.33 | 17.62 | 21.57 | 21.57 | 0.017 | 1.857 | 3.809 | 3.809 |
| | 300 | 5.11 | 16.03 | 20.69 | 20.69 | 0.023 | 2.651 | 5.342 | 5.342 |
| | 400 | 4.95 | 14.62 | 19.93 | 19.93 | 0.028 | 3.253 | 6.468 | 6.468 |
| | 500 | 4.80 | 13.39 | 19.25 | 19.25 | 0.032 | 3.696 | 7.268 | 7.268 |

From Tables 4-6, it is obvious that the calculated values of the relaxation time ($\tau_{th}$) are of the pico second order, which determines the semiconducting nature of DyX. The thermal relaxation time is maximum along <100> at 100K and it decrease on increasing temperature for all dysprosium monochalcogenides along all directions. At higher temperatures the trend in decrement is slow and tends to nearly constant. Thus, at 100K temperature and along <100> direction is most suitable for phonons to restore its original position distorted due to ultrasonic waves propagation. The thermal relaxation time is a key factor for the calculation of ultrasonic attenuation. The acoustic coupling constant decides the conversion of acoustic energy to thermal energy and vice-versa. From Tables 4-6 it is obvious that the $D_L$>$D_S$ which indicates that the longitudinal wave converted more energy than the shear wave for DyX. Again, for shear wave the acoustic coupling constant is maximum along <110> for DyS, DySe and DyTe in $B_1$ phase. This shows that exchange of ultrasonic energy into thermal energy is maximum along <110>. The values of acoustic coupling constants are compared with

existing results of platinum group metal carbides RhC, PdC and IrC [40]. The values of acoustic coupling constants are decreasing with temperature which decreases conversion of ultrasonic energy to thermal energy. The achieved results of ultrasonic attenuation over the frequency squared due to thermoelastic relaxation mechanism $(\alpha/\nu^2)_{th}$ is smaller than due to Akhieser damping $(\alpha/\nu^2)_{Akh}$ $(=(\alpha/\nu^2)_L+(\alpha/\nu^2)_S)$ under assumption $\omega\tau \leq 1$. It is obvious that ultrasonic attenuation at any temperature depends on materials thermal relaxation time, ultrasonic velocity and coupling constant. It has been found from Tables 4-6 that thermal attenuation increases with increasing temperature and is maximum along <110> and minimum along <100> for all dysprosium monochalcogenides which is comparable with the previous results of similar material [31]. The thermal attenuation is largest for DyTe along <110> and <111> direction at 500K, which shows that ultrasonic energy to thermal energy conversion time is highest for DyTe. Ultrasonic Akhieser loss due to phonon-phonon interaction expands with rising temperature and is highest along <110> which is similar to existing results of [32, 33]. It is obvious from Tables 4-6 that Akhieser loss is very much higher than thermoelectric loss. The ultrasonic attenuation for longitudinal wave $(\alpha/\nu^2)_L$ is higher than that of shear wave $(\alpha/\nu^2)_S$ for DyX. Thus, the Akhieser attenuation is predominant to total attenuation for DyS, DySe and DyTe along <100>, <110> and <111> in temperature range 100-500K. This type of behaviour prevails in semiconducting nature of DyX [2] which justifies the semiconducting nature of DyX.

The total ultrasonic attenuation for the chosen materials with in temperature range 100-500K along each directions i.e. $(\alpha/\nu^2)_{total} = (\alpha/\nu^2)_{th} + (\alpha/\nu^2)_{Akh}$ is shown in Figure 1.

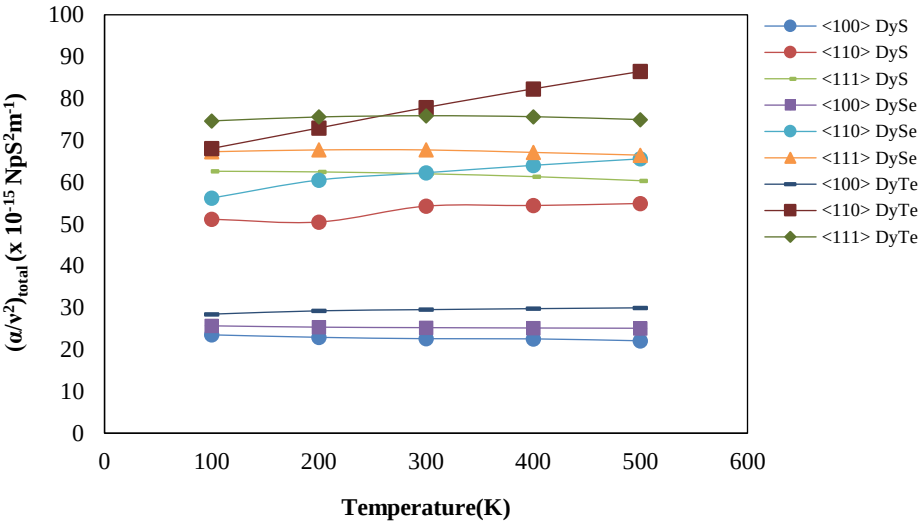


**Figure 7** Temperature dependent total ultrasonic attenuation of DyX along <110>, <110> and <111>

From Figure 7 it is clear that the total ultrasonic attenuation for dysprosium monochalcogenides is minimum along <100> and at 100K which confirms <100> is most appropriate direction for wave propagation. The value of ultrasonic attenuation increases from DyS to DyTe along <100> to <111>. This type of trend has been found very similar to lanthanum monochalcogenides [32].

## 4. Conclusions

On the basis of outcomes of present investigation and their discussions, it is concluded that:

The theory applied for evaluation of orientation and temperature dependent elastic, thermophysical and ultrasonic characteristics of $B_1$ type dysprosium monochalcogenides have been validated and discussed successfully within temperature range 100-500K. The characteristics of the second- and third-order elastic constants are comparable to similar materials of B1 structured. The mechanical constants are largest for DyS which shows DyS is harder and stiffer than DySe and DyTe. The Zener anisotropic factor shows that chosen materials are anisotropic in nature. Cauchy's relation holds good for SOECs at 0K due to absence of vibration energy and deviates at higher temperature (100-500K) for the chosen dysprosium monochalcogenides. The Born stability criterion for mechanical stability has been satisfied for DyS, DySe and DyTe. The calculated values of Cauchy's pressure and Pugh's indicator have verified the brittle nature of the DyX materials in present investigation. The acoustic velocities increase with temperature and the most suitable direction of ultrasonic wave propagation is <100> for selected material DyX. The relaxation time is of the order of pico second with in temperature range 100-500K which shows semiconducting nature of dysprosium monochalcogenides. The attenuation due to thermoelastic mechanism is negligible in comparison to attenuation loss due to Akheiser mechanism at all temperatures for the DyX. The longitudinal coupling constant ($D_L$) is greater than the shear coupling constant ($D_S$) which indicates that ultrasonic energy to thermal energy conversion for shear wave is less in comparison to longitudinal wave within temperature range 100-500K. Ultrasonic attenuation along longitudinal mode dominates over shear mode in case of Akhieser attenuation with in temperature range 100-500K for each direction. The most appropriate direction of acoustic wave propagation is <100> because of lowest ultrasonic attenuation values. The total ultrasonic attenuation loss has been found maximum for DyTe and is minimum for DyS which shows metallic character increases from DyS to DyTe.

The obtained results of dysprosium monochalcogenides DyX provide future aspects to the investigators for further studies as well as this study will be very useful for engineering applications in industries.

## 5. References

[1] Petit L, Szotek Z, Lüders M, Svane A. Rare-earth pnictides and chalcogenides from first-principles. J Phys Condens Matter. 2016;28:223001.

[2] Tripathi SN, Srivastava V, Pawar H, Sanyal SP. First-principles investigation of structural, electronic and mechanical properties of some dysprosium chalcogenides, DyX (X=S, Se and Te). Indian J Phys. 2020;94:1195-201.
[3] Hulliger F, Landolt M, Schmelczer R. Low-temperature behavior of DyS, DySe, HoS and HoSe. In: McCarthy GJ, Silber HB, Rhyne JJ, Kalina FM, editors. The Rare Earths in Modern Science and Technology. Boston: Springer; 1982. p. 455-8.
[4] Schoenes J, Repond P, Hulliger F, Ghosh DB, De SK, Kunes J, et al. Experimental and theoretical investigation of optical properties of dysprosium monopnictides. Phys Rev B. 2003;68(8):085102.
[5] Gaith M. Elastic and mechanical investigation of rare earth monochalcogenides under high pressure. Int Rev Mech Eng. 2020;14(11):693-8.
[6] Bhajanker S, Srivastava V, Sanyal SP. High pressure effect on structural, elastic and thermal properties of DyP and DyAs. J Phys Conf Ser. 2012;377:012079.
[7] Bafekry A, Faraji M, Fadlallah MM, Jappor HR, Hieu NN, Ghergherehchi M, et al. Prediction of two dimensional bismuth-based chalcogenides Bi2X3 (X=S,Se,Te) monolayers with orthorhombic structure: a first-principle study. J Phys D Appl Phys. 2021;54:395103.
[8] Kuroda MA, Jiang Z, Povolotskyi M, Klimeek G, Newns DM, Martyna GJ. Anisotropic strain in SmSe and SmTe: implications for electronic transport. Phys Rev B. 2014;90:245124.
[9] Otero-Díaz LC, Torralvo MJ, Rojas RM. Thermal behaviour and microstructural characterization of γ-Dy2S3. Solid State Ion. 1993;63-65:318-24.
[10] Pokrzywnicki S. Crystal field effects and magnetic properties of Dy2Te3. J Alloys Compd. 1995;225(1-2):163-5.
[11] Khot SD, Malavekar DB, Bagwade PP, Nikam RP, Lokhande CD. Synthesis of reduced graphene oxide (γ GO)/dysprosium selenide (Dy2S3) composite electrode for energy storage; flexible asymmetric super capacitor. J Phys Chem Solids. 2023;179:111419.
[12] Privitera SMS. Synthesis, properties and applications of germanium chalcogenides. Nanomaterials. 2022;12(17):2925.
[13] Ning S, Huang S, Zhang T, Zhang Z, Qi N, Chen Z. Two dimensional β-PdX2 (X= S, Se,Te) monolayers with promising potential for thermoelectric applications. J Phys Chem C. 2022;126(42):17885-93.
[14] Singh D, Yadav RR, Tiwari AK. Ultrasonic attenuation in semiconductors. Indian J Pure Appl Phys. 2002;40:845-9.
[15] Lahourpour F, Boochani A, Parhizgar SS, Elahi SM. Structural, electronic and optical properties of graphene-like nano-layers MOX2 (X: S, Se, Te): DFT study. J Theor Appl Phys. 2019;13:191-201.
[16] Srivastava V, Bhajanker S, Sanyal SP. High pressure effect on structural and mechanical properties of some LnO (Ln = Sm, En, Yb) compounds. Phys B Condens Matter. 2011;406(11):2158-62.
[17] Dantas NS, da Silva AF, Persson C. Electronic band-edge properties of rock salt PbY and SnY(Y=S,Se and Te). Opt Mater. 2008;30(9):1451-60.
[18] Li XH, Xing CH, Cui HL, Zhang RZ. Elastic and acoustical properties of Cr3AlB4 under pressure. J Phys Chem Solids. 2019;126:65-71.
[19] Shafiq M, Arif S, Ahmad I, Asadabadi SJ, Maqbool M, Aliabad HAR. Elastic and mechanical properties of lanthanide monoxides. J Alloys Compd. 2015;618:292-8.
[20] Winey JM, Hmiel A, Gupta YM. Third-order elastic constants of diamond determined from experimental data. J Phys Chem Solids. 2016;93:118-20.
[21] Liu L, Xu G, Wang A, Wu X, Wang R. First-principles investigations on structure stability, elastic properties, anisotropy and Debye temperature of tetragonal LiFeAs and NaFeAs under pressure. J Phys Chem Solids. 2017;104:243-51.
[22] Born M, Mayer JE. Zur Crittertheorie der Ionenkristalle. Zeitschrift für Physik. 1932;75:1-18. (In German)
[23] Singh A, Singh D. Investigation of alkali halide crystals AX (A= Li, Na, K; X= F,Cl, Br) by elastic, mechanical and ultrasonic analysis. Zeitschrift für Naturforschung A. 2023;78(10):947-58.
[24] Bhalla V, Singh D. Mechanical and thermo-physical properties of rare-earth materials. In: Aswal DK, Yadav S, Takatsuji T, Rachakonda P, Kumar H, editors. Hand book of Meterology and Applications. Singapore: Springer; 2022. p. 1-33.
[25] Tripathi S, Agrawal R, Singh D. Non-linear elastic, ultrasonic and thermophysical properties of lead telluride. Int J Thermophys. 2019;40:78.
[26] Singh D, Tripathy C, Paikaray R, Mathur A, Wadhwa S. Behaviour of ultrasonic properties on SnAs, InTe and PbSb. Eng Appl Sci Res. 2019;46(2):98-105.
[27] Akhieser A. On the absorption of sound in solids. J Phys (Moscow). 1939;1(1):277-87.
[28] Bömmel HE, Dransfeld K. Excitation and attenuation of hypersonic waves in quartz. Phys Rev. 1960;117(5):1245-52.
[29] Mason WP. Effect of impurities and phonon processes on the ultrasonic attenuation of germanium, crystal quartz, and silicon. Phys Acoust. 1965;3:235-86.
[30] Tosi MP. Cohesion of ionic solids in the Born model. Solid State Phys. 1964;16:1-120.
[31] Singh D, Pandey DK, Singh DK, Yadav RR. Propagation of ultrasonic waves in neptunium monochalcogenides. Appl Acoust. 2011;72(10):737-41.
[32] Yadav RR, Singh D. Ultrasonic attenuation in lanthanum monochalcogenides. J Phys Soc Jpn. 2001;70:1825-32.
[33] Yadav RR, Singh D. Effect of thermal conductivity on ultrasonic attenuation in praseodymium monochalcogenides. Acoust Phys. 2003;49:595-604.
[34] Bala J, Singh D. Elastic and ultrasonic properties of fermium monopnictides. Eng Appl Sci Res. 2020;47(2):182-9.
[35] Cousins CSG. New relation between elastic constants of different orders under central force interactions. J Phys C: Solid State Phys. 1971;4:1117.
[36] Pugh SF. XCII. Relations between the elastic moduli and the plastic properties of polycrystalline pure metals. Lond Edinb Dubl Phil Mag. 1954;45(367):823-43.
[37] Pettifor DG. Theoretical predictions of structure and related properties of intermetallic. Mater Sci Technol. 1992;8(4):345-9.
[38] Watt JP. Elastic properties of polycrystalline minerals: comparison of theory and experiment. Phys Chem Minerals. 1988;15:579-87.
[39] Gray DE. American Institute of Physics Handbook, 3rd ed. New York: McGraw–Hill; 1972.
[40] Singh A, Singh D. Influence of temperature and orientation on elastic, mechanical, thermophysical and ultrasonic properties of platinum group metal carbides. Johnson Matthey Technol Rev. 2024;68(1):49-59.